JOURNAL OF CATALYSIS 46, 372–381 (1977)

Nonuniform Distribution of Catalysts on Supports

II. First Order Reactions with Poisoning

E. ROBERT BECKER[1] AND JAMES WEI

Department of Chemical Engineering, University of Delaware, Newark, Delaware 19711

Received May 20, 1976; revised December 9, 1976

Catalysts with the same quantity of active material, deposited in different manners on supports and subjected to a period of poison deposition, are compared in their durabilities towards poisoning. Catalyst spheres with an exterior distribution are optimum when poison distributes uniformly. An interior catalyst distribution is optimum when poison concentrates at the pore mouth, and when the main reaction experiences little diffusion limitation. A criterion for catalyst selection is given, based on durability and efficiency.

NOMENCLATURE

a_c	Catalyst surface area [cm²/g]
c	Concentration [g moles/cm³]
c_w	Surface poison concentration [g moles/cm²]
$\bar{C}$	Cumulative emission of pollutants [g moles]
D	Effective diffusion coefficient [cm²/sec]
D_p	Particle diameter [cm]
F	Flow rate (cm³/sec]
k	First order rate constant [1/sec]
P	Poison precursor compound
r	radial distance in catalyst sphere [cm]
R	Radius of catalyst support sphere [cm]
$\Re$	Average rate of poison deposition [g moles/cm³ sec]
$\Re^*$	Average rate of poison deposition, dimensionless
S	Selection criterion
t	Time [sec]
T	Age of Catalyst
V_c	Volume of catalyst [cm³]
W	Surface poison compound
x	r/R, dimensionless radial distance
y	c/c_s, dimensionless concentration
y_w	$a_c c_w/c_{ps}\ \theta\rho_c$, dimensionless surface poison concn
α_p	Surface covered by poison [cm²/g mole]
η	Effectiveness factor defined by Eq. (16)
θ	Catalyst porosity [cm³ void/cm³ catalyst]
λ	$\rho_c\alpha_p\theta c_{ps}/a_c$, dimensionless constitutive coefficient
ρ_c	Density of catalyst particle [g/cm³]
τ	tD_p/R^2, dimensionless time
$\tau_{0.4}$	Time elapsed for η to reach 0.4
ϕ	First order Thiele modulus
χ	Fractional CO conversion
ψ_m	$R(k_m/D_m)^{\frac{1}{2}}$, Thiele parameter

Subscripts

av	average
c	catalyst
m	main reaction
p	poison precursor

[1] Present address: Chemical Engineering Research Group, C.S.I.R., P.O. Box 395, Pretoria 0001, South Africa.

ISSN 0021-9517

s particle surface
w surface poison

Superscripts

0 initial state

INTRODUCTION

Impurities in chemical feedstocks play an important role in catalyst deactivation. Compounds of sulfur, nitrogen, vanadium, nickel and lead are notorious for their strong poisoning of hydrodesulfurization and oxidation catalysts. The lead levels in gasoline have to be lowered by two orders of magnitude to protect the automotive catalyst from premature failure.

On examination of the deactivated catalysts, one often finds the poison compounds concentrated in a narrow band or shell near the surface of the catalyst particle. McArthur (*1*, *2*) published two studies of poison distributions in automotive catalysts. He found that the sulfur and lead concentrations were highest at the particle exterior, decreasing hyperbolically towards the particle interior. McArthur's sulfur electron microprobe profiles are replotted in Fig. 1 for two temperatures. At the higher temperature of 1250°F the sulfur profile is steeper than at 1000°F, which suggests a diffusion limited poison reaction. Hegedus and Baron (*3*) and Su and Weaver (*4*) found similar pore mouth poisoning behavior of lead in noble metal and base metal oxide catalysts. Sato *et al.* (*5*) reported data which showed that vanadium compounds deposit preferentially on the outside of cobalt–molybdenum catalyst while nickel penetrates the entire particle.

The question that arises from such data is whether one might be able to design more poison-resistant catalyst particles by distributing the catalytic material in such a way so as to protect it from the poison layers. It may be advantageous to tolerate a certain degree of diffusion resistance in order to avoid rapid deactivation by poisoning. In part I (*11*) of this work, performance features of interior catalyst layers were demonstrated for reactions with strong reactant inhibition. This part of the study analyzes the effect of nonuniform distribution of catalyst in a sphere where the main reaction is first order and the catalyst is poisoned by impurities in the feed. Whereas an "egg shell" distribution is clearly optimum in the absence of pison and selectivity considerations, an interior layer of catalyst may well have advantages when the catalyst is poisoned.

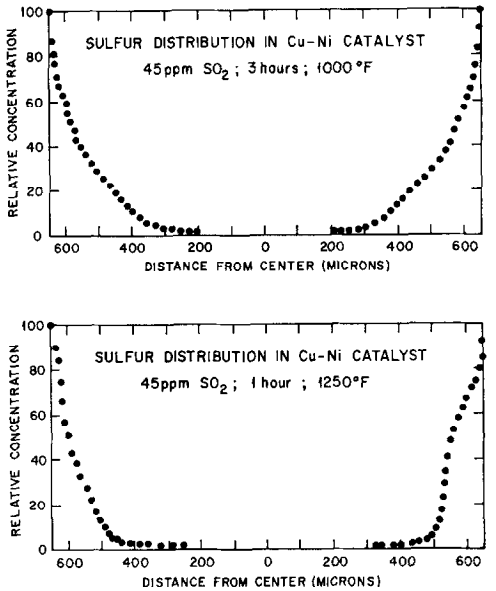

FIG. 1. Sulfur distribution in a copper–nickel catalyst from data by McArthur (*1*).

MODE OF CATALYST DISTRIBUTION

For the purpose of this analysis, one third of the volume of a support sphere is impregnated with catalytic material. Equal quantities of catalyst are concentrated in the regions shown in Fig. 2. This mode of distribution ensures a constant dispersion of active material in the three nonuniform catalyst distributions. The outer or "egg shell" catalyst has an active shell penetrating to 0.13 of the sphere radius. The middle or "egg white" catalyst has an inert core

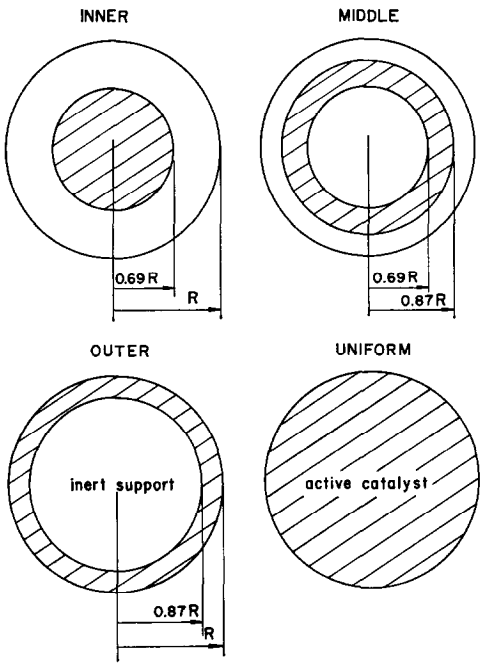

FIG. 2. Nonuniform distribution of catalytic material in a sphere.

and shell, whereas the inner or "egg yolk" catalyst has an active core with a thick inert support shell.

Ideally one may regard the thickness and the depth of the catalyst layer as independent design variables. The method of analysis is not restricted to the chosen distributions. The three layer mode of distribution suffices to demonstrate the performance characteristics of extremes in catalyst location.

IMPURITY POISONING MODEL

The fundamental steps in poison reactions are complex and are not well understood. Butt (*6*) has reviewed the common empirical models which simulate the overall decrease in activity of a catalyst. Elemental analysis by electron microprobe scanning promises to be a useful tool in formulating and understanding the poisoning process. Poison compound profiles in catalyst particles, such as those shown in Fig. 1, are useful in modeling the poisoning reaction.

The poison molecules can interact with the catalyst in various ways. At one end of the spectrum one may envisage poison molecules which react with or adsorb on active sites only, reaching some equilibrium concentration. This would be termed selective saturation poisoning. At the other end of the spectrum, one may imagine a random deposition of poison molecules on a surface with no site preference and no saturation concentration. This can be termed nonselective poison deposition.

Hegedus and Baron (*3*) and McArthur (*1*, *2*) found no site preference of lead on their respective catalysts. The lead and sulfur poison profiles in the literature (*1–5*) do not indicate a saturation concentration of poison on the catalyst surface, although Hegedus and Baron suggested that there may well be a saturation level of lead corresponding to a monolayer of molecules on the surface.

The simple model proposed here assumes no saturation and no selectivity for sites on the surface. The poison centrations are also taken to be low enough so as not to affect the diffusivities of the chemical species present. This would rule out the effect of pore mouth plugging as in hydrodesulfurization catalysts which are exposed to high metal concentrations in the feed. Hegedus (*7*) demonstrated that in automotive noble metal oxidation catalysts, the transport properties are not significantly affected.

The shape of the poison profiles in the literature (*1–4*) is hyperbolic, decreasing from the surface inwards. The curves are similar to concentration profiles of reactants under diffusional influence with first order reaction. Consider the reaction of poison precursor (P) to poison (W) at the surface.

$$P \rightarrow W.$$

For a first order poison deposition process without saturation, the poison rate is given by:

$$\Re_p = k_p c_p. \qquad (1)$$

A constitutive equation is needed to relate the first order rate constant of the catalyst for the main reaction to the amount of poison on the surface. For a random deposition this can be shown (*8*) to be:

$$k_m = k_m^0 \exp(-\alpha_p c_w), \qquad (2)$$

α_p is the constitutive coefficient. The Thiele modulus for the poison reaction is defined by:

$$\phi_p = R(k_p/D_p)^{\frac{1}{2}}, \qquad (3)$$

and the concentration profile of poison precursor in the spherical particle is given by:

$$c_p = \frac{c_{ps} \sinh(\phi_p r/R)}{(r/R)\sinh\phi_p}. \qquad (4)$$

The average rate of poison deposition in the active volume of the support sphere is expressed as:

$$\Re = \int_{r_1}^{r_2} k_p c_p 4\pi r^2 dr \Big/ \int_{r_1}^{r_2} 4\pi r^2 dr.$$

Multiplication of $\Re$ by $R^2/D_e c_{ps}$ yields a dimensionless poison rate $\Re^*$:

$$\Re^* = \int_{r_1}^{r_2} \phi_p^2 (c_p/c_{ps}) 4\pi r^2 dr \Big/ \int_{r_1}^{r_2} 4\pi r^2 dr. \qquad (5)$$

$\Re^*$ is plotted as a function of ϕ_p in Fig. 3 for the four catalyst particles shown in Fig. 2. When poison deposits uniformly, ϕ_p is low and all catalysts are poisoned at the same rate as expected. As diffusion becomes the rate limiting step in the process, ϕ_p is high and the poison deposits preferentially on the outer layer of the particle. The inner layer catalysts are protected from the poison, which is seen as a decrease in poison deposition rate with increasing ϕ_p. At a value of ϕ_p of 10 the "egg shell" catalyst poisons at nearly four times the rate of the "egg white," and more than 25 times the rate of the "egg yolk" catalyst.

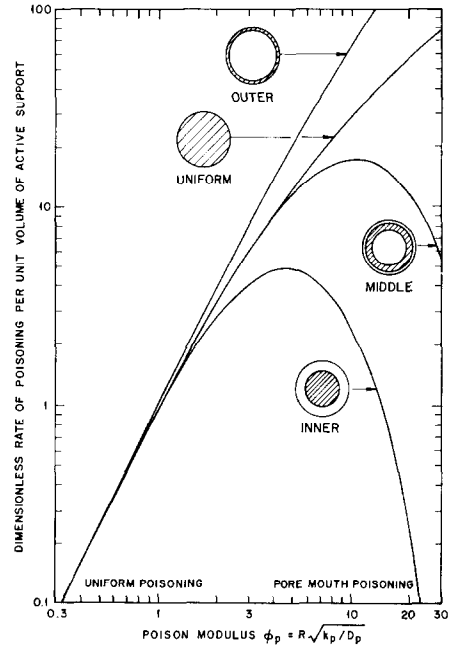

FIG. 3. First order poison deposition rates in non-uniformly distributed catalyst particles.

FIRST ORDER REACTION WITH POISONING

So far only the poison reaction has been considered. To make a choice of catalyst design, it is necessary to determine the influence of catalyst distribution on the performance of the main reaction in the presence of poison deposition. A first order main reaction is modeled in this work.

The deactivation time is much slower than transients of the main reaction. Quasi steady-state can thus be reasonably assumed for the main reaction, denoted by subscript m. A mass balance for the components in the support sphere yields:

Main reaction:

$$D_m\left(\frac{d^2c_m}{dr^2} + \frac{2}{r}\frac{dc_m}{dr}\right) = k_m(t, r)c_m. \qquad (6)$$

Poison reaction:

$$D_p\left(\frac{d^2c_p}{dr^2} + \frac{2}{r}\frac{dc_p}{dr}\right) = k_p c_p. \qquad (7)$$

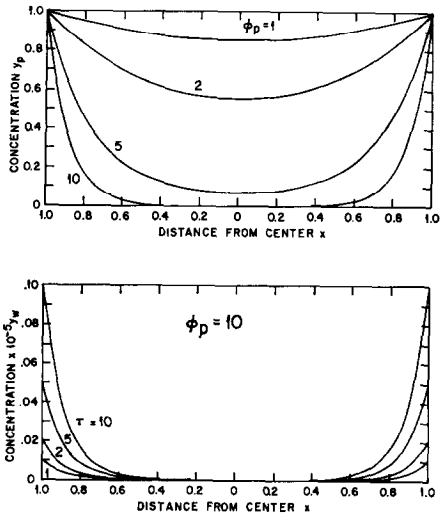

FIG. 4. Poison precursor profiles and poison deposit build-up in a sphere for first order poison deposition.

Poisson accumulation:

$$\frac{a_c}{\rho_c\theta}\frac{\partial c_w}{\partial t} = k_p c_p, \tag{8}$$

with the system boundary conditions:

$$\begin{aligned} c_m &= c_{ms} \quad \text{at} \quad r = R, \\ c_p &= c_{ps} \quad \text{at} \quad r = R, \\ dc_m/dr &= 0 \quad \text{at} \quad r = 0, \\ dc_p/dr &= 0 \quad \text{at} \quad r = 0, \\ c_w(r) &= 0 \quad \text{at} \quad t = 0. \end{aligned}$$

The rate constant k_m is related to the poison concentration c_w by Eq. 2. The equations are reduced to dimensionless form by introducing the parameters:

$$\begin{aligned} x &= r/R; & y_m &= c_m/c_{ms}, \\ y_p &= c_p/c_{ps}; & y_w &= a_c c_w/(c_{ps}\theta\rho_c), \\ \tau &= tD_p/R^2; & \phi_p &= R(k_p/D_p)^{\frac{1}{2}}, \end{aligned}$$

and

$$\psi_m(x, \tau) = R[k_m(x, \tau)/D_m]^{\frac{1}{2}}.$$

Equations (6) through (8) in dimensionless form are:

$$y_m'' + (2/x)y_m' = \psi_m^2(x, \tau)y_m, \tag{9}$$

$$y_p'' + (2/x)y_p' = \phi_p^2 y_p, \tag{10}$$

$$\partial y_w/\partial\tau = \phi_p^2 y_p, \tag{11}$$

with boundary conditions:

$$\begin{aligned} &y_m(1, \tau) = 1, \\ &y_p(1, \tau) = 1, \\ &y_m'(0, \tau) = 0, \\ &y_p'(0, \tau) = 0, \\ &y_w(x, 0) = 0, \\ &\psi_m(x, \tau) = \psi_m(x, 0)\exp(-\lambda y_w(x, \tau)/2), \end{aligned} \tag{12}$$

where $\lambda = \rho_c\alpha_p\theta c_{ps}/a_c$.

The poison precursor (P) profile, given by Eq. (4), is calculated by integrating Eq. (10). In terms of the reduced variables it is written as:

$$y_p = \sinh(\phi_p x)/x \sinh\phi_p. \tag{13}$$

Integration of Eq. (11) yields the surface poison (W) concentration.

$$y_w(x, \tau) = \phi_p^2\tau \sinh(\phi_p x)/x \sinh\phi_p. \tag{14}$$

The activity within the sphere is prescribed by combining Eqs. (12) and (14):

$$\psi_m(x, \tau) = \psi_m(x, 0) \times\exp\left[-\frac{\lambda \sinh(\phi_p x)}{2x \sinh\phi_p}\phi_p^2\tau\right]. \tag{15}$$

Poison precursor profiles for ϕ_p = 1, 2, 5, and 10 and the deposited poison concentration when ϕ_p = 10 at several times are shown in Fig. 4.

The remaining task is to solve Eq. (9) with an appropriate numerical integration. A piecewise linearization of the right side of Eq. 9 results in a set of coupled ordinary differential equations. These can be efficiently solved by a matrix scheme to yield the concentration profile and concentration gradient of the main reactant. The details

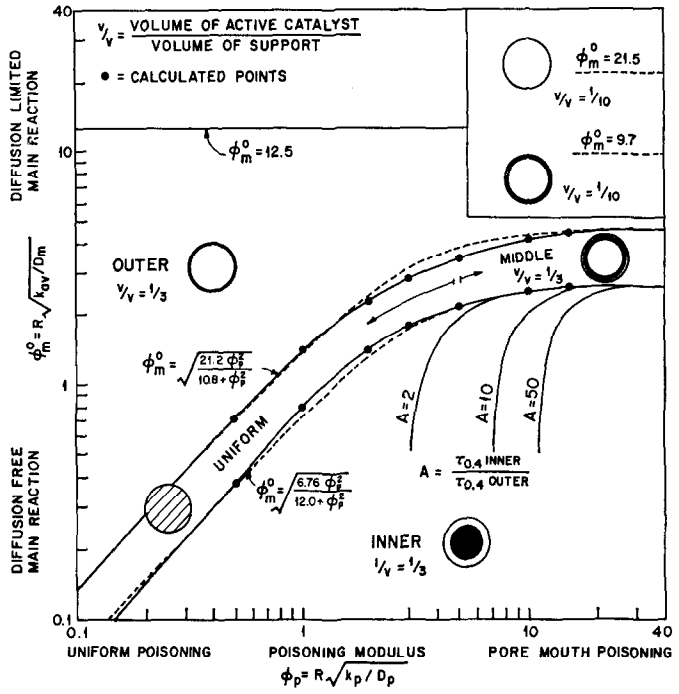

FIG. 5. Catalyst selection chart for four catalyst designs based on a criterion of longest useful life.

of the integration may be found elsewhere (*8*).

The effectiveness factor of the main reaction is time dependent. It includes both diffusion and poison effects.

$$\eta(t) = \frac{4\pi R^2 D_m (dc_m/dr)\,|_{R,t}}{c_{ms}\int_0^R 4\pi r^2 k_m{}^0(r)dr}. \qquad (16)$$

The reference efficiency of unity refers to fresh catalyst in the absence of diffusion. A Thiele modulus for the nonuniformly impregnated support pellets is defined by taking an average value of the rate constant over the entire support sphere, k_{av}.

$$(\phi_m{}^0)^2 = \frac{R^2}{D_m}\int_0^1 \frac{4\pi x^2 k_m(x,0)dx}{4\pi/3} \equiv \frac{R^2 k_{av}}{D_m}. \qquad (17)$$

In reduced form the effectiveness factor is written as:

$$\eta(\tau) = \frac{3(dy_m/dx)\,|_{1,\tau}}{(\phi_m{}^0)^2}. \qquad (18)$$

In each calculation ϕ_p and $\phi_m{}^0$ are fixed and η is calculated for uniform, egg shell, egg white and egg yolk catalysts at several times. The effectiveness factors are then mapped as functions of time. Calculations were performed for uniform to pore mouth poisoning, $0.2 \leq \phi_p \leq 20$, in combination with diffusion-free to diffusion-limited main reaction, $0.1 \leq \phi_m \leq 12$. The resulting curves are numerous. Representative examples are reported elsewhere (*8*) together with the FORTRAN program.

CATALYST SELECTION

The effectiveness factor is a function of five variables: ϕ_p, $\phi_m{}^0$, time, catalyst distribution and the poison precursor concen-

tration, c_{ps}. The last two variables are combined in the dimensionless time parameter $\lambda\tau$.

$$\eta = \eta(\text{catalyst distribution}, \phi_p, \phi_m{}^0, \lambda\tau). \tag{19}$$

A simple criterion for catalyst selection can be taken to be the time elapsed before the effectiveness factor drops to a predetermined value, 0.4, say. This constitutes a catalyst choice based on the longest useful life, $\tau_{0.4}$, under one set of operating conditions. The values of ϕ_p, $\phi_m{}^0$ and catalyst distribution are fixed, and the time taken to reduce initial efficiency to 0.4 by poisoning is calculated. The catalyst with the longest "life time," $\tau_{0.4}$, is optimum for that combination of ϕ_p and $\phi_m{}^0$. A catalyst selection chart based on the catalyst distributions in Fig. 2 is shown in Fig. 5.

In the lower right region of the $\phi_p - \phi_m{}^0$ plane, the inner or egg yolk catalyst is preferred since the poison deposits in the "egg shell" layer of the support particle. The lines of constant A value are iso-advantage lines, comparing the life of the egg yolk catalyst to that of the egg shell catalyst. When the main reaction has an initial Thiele modulus of one, for instance, and the poison modulus has a value of 11.5, corresponding to severe port mouth poisoning, the inner catalyst lasts 50 times as long as the egg shell catalyst. As the main reaction becomes diffusion limited, the effectiveness of the fresh catalyst drops below 0.4. For the inner catalyst the limiting value of $\phi_m{}^0$ is 2.6. The middle catalyst has a maximum operating modulus of 4.6, and the outer catalyst operates up to $\phi_m{}^0$ of 12.5 according to the chosen criterion. Above a value of $\phi_m{}^0 = 12.5$, all these catalysts have an initial effectiveness below 0.4. The upper left region of the plot corresponds to severely diffusion limited main reaction in combination with uniform poisoning. In this region the egg shell catalyst holds the advantage since all catalysts are poisoned at the same rate (see also Fig. 3), yet the egg shell catalyst offers the least diffusion resistance to reaction.

The three-layer mode of distribution can be extended to other modes of distribution. If one distributes the catalytic material in adjacent layers occupying one tenth of the support volume, the outermost layer will tolerate diffusion resistance up to $\phi_m{}^0$ of 21.5. The next-to-outermost layer can operate above effectiveness 0.4 up to $\phi_m{}^0$ of 9.7. The broken lines in the upper right region of Fig. 5 show these limiting values. From this simple criterion, the best choice of catalyst distribution is the one which is barely protected from the poison layer and offers a minimum of diffusion resistance to the main reaction. The boundaries between the regions of optimum catalyst distribution are fitted by the broken line curves:

$$\phi_m{}^0 = [21.2\phi_p{}^2/(10.8 + \phi_p{}^2)]^{\frac{1}{2}} = f_1(\phi_p), \tag{20}$$

and

$$\phi_m{}^0 = [6.76\phi_p{}^2/(12.0 + \phi_p{}^2)]^{\frac{1}{2}} = f_2(\phi_p). \tag{21}$$

In algebraic terms the selection rule is given by:

Outer: $f_1(\phi_p) \leq \phi_m{}^0 < 12.5$, $0.1 < \phi_p < 40.$

Middle: $f_2(\phi_p) < \phi_m{}^0 < f_1(\phi_p)$, $5 < \phi_p < 40.$

Uniform: $f_2(\phi_p) < \phi_m{}^0 < f_1(\phi_p)$, $0.1 < \phi_p < 5.$

Inner: $\phi_m{}^0 \leq f_2(\phi_p)$, $0.1 < \phi_p < 40.$

In many catalyst systems the operating conditions will not be kept constant as deactivation occurs. In reforming, for instance, the temperature is increased as the catalyst deactivates to maintain constant production levels. When the compensating temperature increases lead to unacceptable selectivity, the catalyst is regenerated.

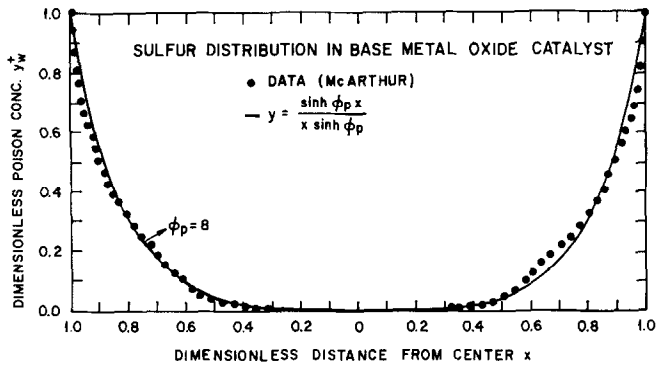

FIG. 6. First order concentration profile fitted to sulfur distribution data of McArthur (*1*).

Such a mode of operation would correspond to a time varying ϕ_p and $\phi_m{}^0$. In this case the above analysis is complicated and difficult to generalize. Calculations can, however, be adapted to suit each particular case.

AUTOMOTIVE CATALYSTS

The performance criterion for automotive catalysts is complicated. Catalyst converters are subjected to a 23 min federal test cycle during which flow rates, inlet concentrations and inlet temperatures vary over wide ranges. The average concentration of emitted pollutants is expressed in grams per mile. This quantity is related to the cumulative emission, $\bar{C}(T)$, a number which depends on catalyst age (*9*).

$$\bar{C}(T) = \int_0^{23} F(t)c_{\text{out}}(t,T)dt. \qquad (22)$$

A catalyst selection criterion may be formulated as:

$$S = \text{Min} \int_0^{t_{\text{total}}} \bar{C}(T)dt, \qquad (23)$$

$$\left\{\begin{matrix}\text{catalyst} \\ \text{distribution}\end{matrix}\right\}$$

t_{total} is the required life of the catalyst corresponding to 50,000 miles of driving. A complete history of flow rate, temperature and concentration would be required to evaluate Eqs. (22) and (23). The calculations can, however, be simplified by two observations:

1. The bulk of pollutants are emitted during the first 2 min of the federal test cycle, while the catalyst is warming up from ambient temperatures (*9*). The conversion of pollutants during this warm-up stage is indicative of the total emissions.

2. After the first few minutes of operation, the catalyst reaches a temperature of 1000–1200°F with few major fluctuations under normal operating conditions. Poisoning of the catalyst can thus be approximated to be isothermal at 1000°F, say.

The conversion of CO is calculated for the four catalyst particles in Fig. 2 at three different times during the life of the catalyst. The flow rate through the converter is typical of idle conditions, of the order of 20 scfm. The fuel contains 0.05 g lead/gal. For a first order reaction the conversion is given by:

$$\chi = 1 - \exp(V_c k_m \eta / F). \qquad (24)$$

Kinetic parameters for transition metal catalysts are taken from Kuo *et al.* (*10*). The poison modulus is calculated by fitting McArthurs' sulfur data at 1000°F. McArthur's data show the lead and sulfur profiles to be parallel. A profile corresponding to ϕ_p of 8 gives a good fit to the data and is shown in Fig. 6.

TABLE 1

Constants for CO-Conversion Calculations

k_{av}	$= 1.78 \times 10^8 \exp(-16{,}100/T^0R)$
D_m	$= 0.06$ cm²/sec
R	$= 0.16$ cm
V_c	$= 3000$ cm³ spherical pellets
F	$= 20$ scfm $= 9439$ cm³/sec (STP)
Space velocity	$= 10{,}000$ hr^{-1}
ϕ_p	$= 8$

The constants for the conversion calculations are summarized in Table 1. External mass transfer considerations were neglected in this initial analysis. Details of the calculation procedure are given elsewhere (*8*).

Three conversion versus temperature plots are shown in Fig. 7. When the catalyst is fresh, $\lambda\tau = 0$, the egg shell catalyst is marginally better than the uniform and middle catalyst. Taking 50% conversion as light-off for reference, the egg shell catalyst lights off at 453°F compared to 457 and 459°F for the uniform and egg white catalyst, respectively. The egg yolk catalyst lights off much later at 483°F. As temperature increases the conversion of the egg yolk catalyst flattens out and approaches

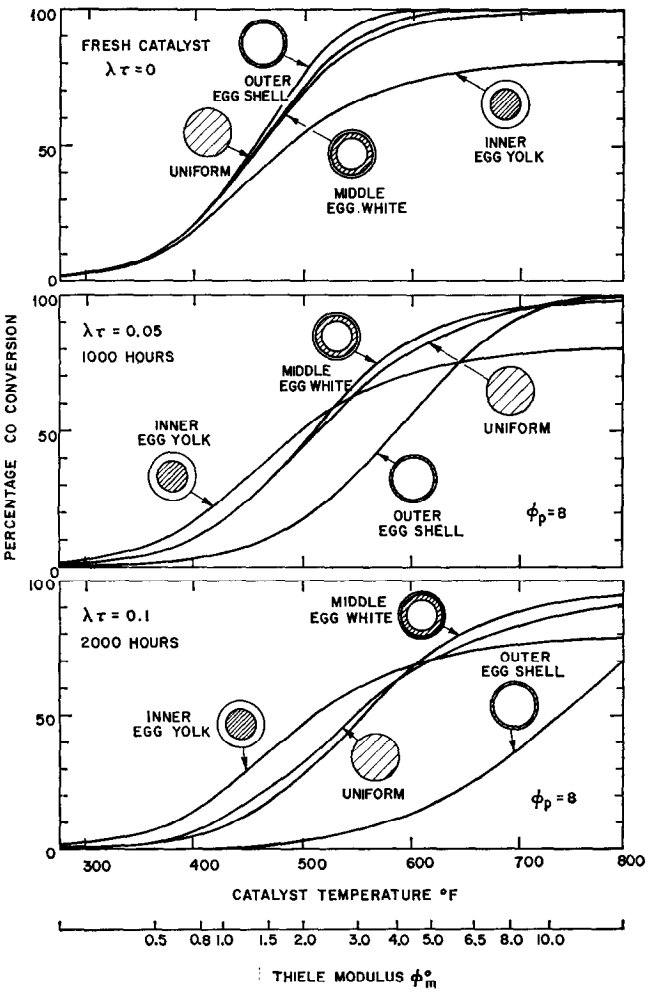

FIG. 7. CO conversion over base metal oxide catalyst at zero, 1000, and 2000 hr of operation with low-lead fuel for inner, middle, uniform and outer catalyst particles.

maximum conversion very slowly. This is a manifestation of the severe diffusion restriction imposed by the thick layer of inert support. The effectiveness factor is proportional to $(\phi_m^0)^{-2}$ in this region of temperature.

After 1000 hr of converter operation the egg shell catalyst has been poisoned considerably, giving 50% conversion at 584°F. The loss of activity due to poisoning in the middle and uniform catalyst is less pronounced. The light-off temperatures are 510 and 514°F, respectively, corresponding to an increase of just over 50°F in light-off temperature. The egg yolk catalyst is virtually unaffected by poisoning.

After 2000 hr of operation the egg shell catalyst is severely poisoned, requiring a 287°F boost to match its fresh performance. This corresponds to a 98% drop in efficiency due to poisoning. The middle and uniform catalysts convert 50% of the inlet CO at roughly 550°F, corresponding to an 80% loss in activity after 2000 hr. The egg yolk catalyst achieves 50% conversion at 510°F, not much different from the fresh state. An integration of the time dependent conversion curves over the life of the catalyst according to Eq. (23) would show the middle or egg white catalyst to be the best choice of the four catalysts under consideration.

DISCUSSION

In part I (*11*) of this work the potential application of interior layer catalysts for bimolecular Langmuir reactions were discussed. The concept of distributing active material in portions of a catalyst support has further application for positive order reactions with poisoning. In situations of severe pore mouth poisoning an interior layer catalyst, such as an egg white or egg yolk catalyst, has substantial potential to increase the poison resistance of the catalyst. Electron microprobe analysis of spent catalysts serves as a useful tool in understanding and modeling the poison deactivation.

Diffusion limitation of the main reaction is not the only determining factor in catalyst particle design when poisons are present. Under uniform poisoning conditions an egg shell catalyst remains optimum, especially when the main reaction is diffusion limited. When poison deposits in the outer shell of a catalyst, an inner layer catalyst can offer substantial improvements over conventional catalyst particles.

ACKNOWLEDGMENTS

This work was supported by NSF Grant GK-38189. We thank Dr. McArthur from Union Oil Co. and Dr. E. Su of Ford Motor Co. for the poison electron microprobe profiles.

REFERENCES

1. McArthur, D. P., presented: Gordon Res. Conf. 1972.
2. McArthur, D. P., *Advan. Chem. Ser.* **143**, 85 (1975).
3. Hegedus, L. L., and Baron, K., presented: joint VDI-AIChE meet., Munich, 1974.
4. Su, E. C., and Weaver, E. E., SAE paper 730594, Automotive Eng. Congr., Detroit, 1973; Su, E. C., personal communication, 1974.
5. Sato, M., Takayama, H., Kurita, S., and Kwan, T., *Nippon Kagaku Zasshi* **92**, 10 (1971).
6. Butt, J. B., *Advan. Chem. Ser.* **109**, 259 (1972).
7. Hegedus, L. L., *J. Catal.* **37**, 127 (1975).
8. Becker, E. R., PhD dissertation, Chem. Eng. Dept., Univ. of Delaware, 1975.
9. Wei, J., *in* "Advances in Catalysis" (D. D. Eley, H. Pines and P. B. Weisz, Eds.), Vol. 24, p. 57. Academic Press, New York, 1975.
10. Kuo, J. C. W., Morgan, C. R., and Lassen, H. G., SAE paper 710289, Automotive Eng. Congr., Detroit, 1971.
11. Becker, E. R., and Wei, J., *J. Catal.* **46**, 365 (1977).